New Phytologist

Research

# Root hairs enable high transpiration rates in drying soils

**Andrea Carminati[1], John B. Passioura[2], Mohsen Zarebanadkouki[1], Mutez A. Ahmed[1,3,4], Peter R. Ryan[2], Michelle Watt[5] and Emmanuel Delhaize[2]**

[1]Chair of Soil Physics, University of Bayreuth, Bauyreuth D-95447, Germany; [2]CSIRO Agriculture and Food, GPO Box 1600, Canberra, ACT 2601, Australia; [3]Division of Soil Hydrology, Georg-August Universität, D-37073, Göttingen, Germany; [4]Department of Agricultural Engineering, Faculty of Agriculture, University of Khartoum, Khartoum North, 13314 Shambat, Sudan; [5]Plant Sciences, Institute of Bio- and Geosciences, Jülich Forschungszentrum, Jülich, D-52425, Germany

Author for correspondence:
*Andrea Carminati*
*Tel: +49 (0)921 552295*
*Email: Andrea.Carminati@uni-bayreuth.de*

Received: *7 May 2017*
Accepted: *21 June 2017*

*New Phytologist* (2017)
**doi**: 10.1111/nph.14715

**Key words:** root hairs, root water uptake, soil hydrology, transpiration, xylem suction.

## Summary

- Do root hairs help roots take up water from the soil? Despite the well-documented role of root hairs in phosphate uptake, their role in water extraction is controversial.
- We grew barley (*Hordeum vulgare* cv Pallas) and its root-hairless mutant *brb* in a root pressure chamber, whereby the transpiration rate could be varied whilst monitoring the suction in the xylem. The method provides accurate measurements of the dynamic relationship between the transpiration rate and xylem suction.
- The relationship between the transpiration rate and xylem suction was linear in wet soils and did not differ between genotypes. When the soil dried, the xylem suction increased rapidly and non-linearly at high transpiration rates. This response was much greater with the *brb* mutant, implying a reduced capacity to take up water.
- We conclude that root hairs facilitate the uptake of water by substantially reducing the drop in matric potential at the interface between root and soil in rapidly transpiring plants. The experiments also reinforce earlier observations that there is a marked hysteresis in the suction in the xylem when the transpiration rate is rising compared with when it is falling, and possible reasons for this behavior are discussed.

## Introduction

Root hairs play an important role in the uptake of soil phosphorus. The most compelling evidence for this, in both pot and field trials, comes from studies of root-hairless mutants and their corresponding wild-types (Bates & Lynch, 2001; Gahoonia & Nielsen, 2003; Haling *et al.*, 2013). It is not yet clear that root hairs play a similar role in water uptake (Marzec *et al.*, 2015).

Indeed, the processes that limit the uptake of water by roots from moderately dry soils are controversial. A seminal paper by Gardner (1960) provided a basic physical framework for describing the flow of water from the bulk soil to the root surface, and its dependence on both the hydraulic properties of the soil and the cylindrical geometry. This model assumed that the hydraulic properties of the rhizosphere were equal to those of the bulk soil and that the root–soil interface was a simple boundary condition, namely, a constant rate of water uptake per unit length of root ($m^3\,m^{-1}\,s^{-1}$). However, subsequent research has uncovered other processes that are of comparable or greater importance, but which remain poorly understood.

For instance, several authors have argued that roots progressively lose hydraulic continuity with the soil as it dries (Huck *et al.*, 1970; Herkelrath *et al.*, 1977; Faiz & Weatherley, 1982; Bristow *et al.*, 1985; Carminati *et al.*, 2013). In addition, a large fraction of roots in the subsoil are found in macro-pores and have poor contact with the soil matrix (White & Kirkegaard, 2010). Although root hairs can bridge the gap between roots and soil, it is not known whether they can take up enough water to affect leaf water potential and transpiration.

Early work by Cailloux (1972) with oats (*Avena sativa*) showed, with the use of a micropotometer, that root hairs of seedlings grown on filter paper took up water. Others have compared root-hairless mutants with the corresponding wild-types to investigate the role of root hairs in water uptake with equivocal findings. Suzuki *et al.* (2003), using a hairless mutant of rice, concluded that root hairs do not contribute to water uptake at the seedling stage. An *Arabidopsis thaliana* line genetically engineered to be root hairless took up less water than the wild-type in hydroponic culture, but the ability to take up water from soil was not assessed (Tanaka *et al.*, 2014). Dodd & Diatloff (2016) found that water uptake by the root-hairless *brb* mutant of barley and wild-type plants grown in drying soil did not differ, and suggested that the mutant might have compensated for its lack of root hairs by developing a large root system (Dodd & Diatloff, 2016). The transpiration rate was not controlled in these experiments, and the authors commented that root hairs could become important under high evaporative demand. Segal *et al.* (2008) used magnetic resonance imaging (MRI) on *brb* and wild-type plants, and saw marked depletion of soil water in the root hair zone, possibly caused by water uptake by root hairs. The data

© 2017 The Authors
*New Phytologist* © 2017 New Phytologist Trust

relied on the calibration of the MR images and assumed that the rhizosphere had the same properties as the bulk soil, which might not have been the case. Furthermore, the effect of the root hairs on the ease of water flow towards the root surface was not investigated, and only a single replicate of each genotype was analyzed. In summary, the role of root hairs in water uptake is equivocal and the existing results are speculative and contradictory.

Our hypothesis is that root hairs take up water from soil, and thereby extend the effective radius of roots to facilitate uptake. This, in turn, would decrease the flow velocity ($m\ s^{-1}$) at the surface of the coaxial cylinder defined by the tips of root hairs where water uptake would begin. For example, for a given uptake of water per unit root length ($m^3\ m^{-1}\ s^{-1}$), if the average length of hairs were equal to three times the radius of the root (and, consequently, the sum of the root radius and hair length were four times greater than the root radius), the velocity of the water entering the zone occupied by the hairs would be one-quarter of that entering a hairless root. This ratio becomes particularly important at high transpiration rates in drying soil, as the hydraulic conductivity of a soil decreases rapidly as its water content falls, such that very large gradients in water pressure may be needed to drive the flow. Lang & Gardner (1970), for example, argued that there would be an absolute limit to the uptake rate of water from soil by roots if the relative decrease in the hydraulic conductivity exceeded the relative increase in the pressure gradient.

Figure 1 illustrates this hypothesis: the left-hand side shows the flows of water and the trajectory of matric potential in the hairy wild-type, and the right-hand side shows the same for the hairless mutant. The identical horizontal blue arrows depict the equal rate of uptake per unit length ($m^3\ m^{-1}\ s^{-1}$). The trajectories of matric potential are identical upstream from this point. Closer to each root, the trajectories change markedly. In the root-hairless mutant, the flow of water continues through the soil to the epidermis, with the slope of the matric potential becoming ever steeper towards the root. In the wild-type, water uptake by root hairs (depicted by the small vertical arrows) diverts the flow from within the soil to within the root hairs, thereby reducing the decrease in matric potential across the soil and reducing the flow velocity. Because (to a first approximation) there is a constant number of root hairs crossing the surface of any notional coaxial cylinder within the root hair zone, their collective transport capacity is independent of the radial distance from the root and is independent of the water content of the soil between them. Therefore, it is likely that, when the soil hydraulic conductivity is low, water can flow more easily within the root hairs than within the soil.

The diameters of root hairs are typically *c.* 10 μm for a wide range of species (Dittmer, 1949), and their vacuoles, which presumably enable the flow of water within them, occupy almost all of the diameter (Peterson & Farquhar, 1996). Hairs are likely to have much greater carrying capacity than a dry soil. The largest water-filled pores in soil at a moderately high matric potential of −100 kPa would have effective diameters of only *c.* 3 μm (Passioura, 2010). As the flow of water through narrow tubes depends on the fourth power of the diameter (*Poiseuille's Law*), a root hair of *c.* three times this diameter would have *c.* 100 times the

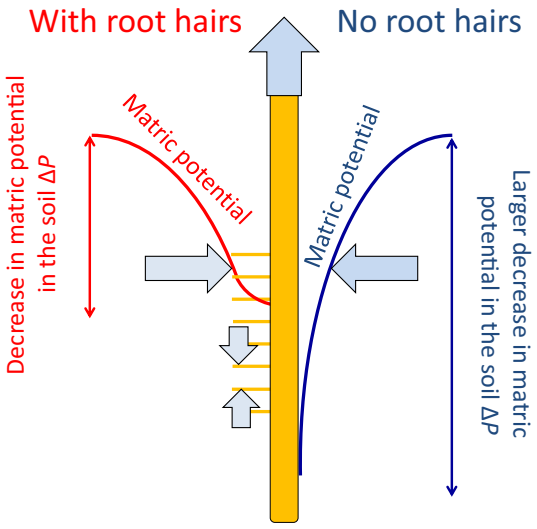


**Fig. 1** Illustration of the hypothetical role of root hairs in facilitating water uptake from the soil. Expected gradients in matric potential around a root with and without hairs for identical rates of water uptake per unit length. Water uptake by root hairs reduces the direct flow of water through the soil into the root epidermis, softening the gradients in water pressure that are expected to develop when transpiration is high and the soil is becoming dry and less hydraulically conductive. The horizontal blue arrows depict the equal rate of uptake per unit length ($m^3\ m^{-1}\ s^{-1}$). Small vertical arrows depict water uptake by root hairs which diverts the flow from within the soil to within the root hairs, thereby reducing the decrease in matric potential across the soil and reducing the flow velocity.

carrying capacity of the largest water-filled pores. Further, flow towards a root through these largest pores would be impeded by the tortuosity of the rest of the pathway and the many bottlenecks along it. Thus, substantial uptake of water by root hairs would largely eliminate the need for direct flow of water through the soil to the root surface, in effect creating an extended root radius for the uptake of water. This, in turn, substantially reduces the difference in matric potential between the bulk soil and the effective root surface.

To test this hypothesis, we grew barley and its root-hairless mutant *brb* in two soils of different hydraulic properties. One soil was a pasteurized synthetic potting mix with high porosity, high water retention and low unsaturated conductivity. The other soil was an un-treated Red Chromosol field soil with lower porosity and higher unsaturated conductivity.

To measure the relationship between the transpiration rate and the pressure drop across the plant and soil, we used the root pressure-chamber method (Deery *et al.*, 2013). This involved: (1) enclosing a pot in a pressure chamber with the shoot enclosed in a cuvette outside the chamber, and (2) systematically varying the transpiration rate ($E$) of the plant, whilst (3) simultaneously monitoring the pressure in the root chamber that was needed to bring a cut in the leaf xylem to the point of bleeding (the 'balancing pressure' $P$). $P$ is numerically equal to the suction that would have existed in the xylem had the roots not been pressurized (Nulsen *et al.*, 1977). The method allowed the hydraulic conductivity of the soil–root–shoot to be measured in intact plants exposed to varying transpiration rates and soil drying. A numerical model of water



© 2017 The Authors
*New Phytologist* © 2017 New Phytologist Trust

flow towards a single root was used to test whether: the measured $P(E)$ relationship is consistent with basic principles of water flow in soils; and the role of root hairs in water uptake could be modeled by extending the effective root radius.

## Materials and Methods

### Germplasm

The spontaneous root-hairless mutant of barley *brb* (*Hordeum vulgare* L. cv Pallas) and its wild-type parent were used in a root pressure chamber to assess water uptake under varying transpiration. The *brb* mutation segregates as a single gene and genetic analyses with molecular markers confirmed the genetic background of *brb* to be the cultivar Pallas (Gahoonia *et al.*, 2001). The rhizosheath, defined as the soil adhering to a plant root, is absent from *brb* (Haling *et al.*, 2010) as shown in Supporting Information Fig. S1(a), with the phenotypes confirming the identity of the lines.

**Soil properties** Plants were grown in either a steam-pasteurized sandy loam potting mix or an un-treated field soil consisting of a Red Chromosol (http://www.clw.csiro.au/aclep/asc_re_on_line/ch/chrosols.htm). The soils were characterized by measuring their water retention and hydraulic conductivities. The water retention was measured using a pressure plate apparatus. The hydraulic conductivity was measured using the evaporation method (Peters & Durner, 2008) and by fitting the measured matric potentials using the Richards equation. The water retention curve and the unsaturated hydraulic conductivity were fitted using the van Genuchten–Mualem parameterization (van Genuchten, 1980) (Methods S1).

The water holding properties of the sandy loam were such as to maintain adequate air-filled porosity throughout a pot despite the bottoms of the pots being saturated after being well watered, as discussed in Passioura (2006). The rationale for using the field soil (Red Chromosol) was that it represented 'reality'. It was not pasteurized and therefore had an active microbial community, together with water holding properties pertinent to field conditions, properties that could lead to chronic waterlogging in a well-watered pot experiment (Passioura, 2006).

### Preparation of pots and plants

Three seedlings of each genotype were grown in the sandy loam potting mix, whereas two seedlings of each genotype were grown in the Red Chromosol. We used cylindrical plastic pots, 86 mm in diameter and 170 mm in height, covered with a 10-mm-thick metal plate with a 5-mm hole in its center into which the roots of a single germinated seed could be inserted (Fig. S1). Once a seedling was established, the hole in the plate was sealed with silicone rubber to form a pressure seal. The pots were initially watered to bring the soil matric potential to *c.* −3 kPa. Once the seedlings were well established, they were transferred to a glasshouse running at *c.* 20°C day temperature and 15°C night temperature until they had three to four fully expanded leaves, at which time they were ready for the experiments (Fig. S1).

### Root pressure chamber

Details of the experimental methods are described in Deery *et al.* (2013) and are summarized here. A pot was placed into the pressure chamber and secured with a flange and bolts. The plant shoot, which remained outside the pressure chamber, was enclosed in a cuvette (Fig. S1c) that had an internal fan to create mildly turbulent air flow at 23°C. The plant was illuminated horizontally by a light-emitting diode (LED) lamp that could be shaded with a mesh screen, and whose distance from the plant was varied to provide a photosynthetic photon flux density ranging from 50 to 600 μmol $m^{-2}$ $s^{-1}$. Air was passed through the cuvette at rates ranging from 1.7 to 3.5 l $min^{-1}$. The humidity of the air was measured with a dewpoint hygrometer (General Eastern Model Dew10-XX1; Billerica, MA, USA) which was switched every 5 min between the air entering the chamber and the air coming out, giving a measurement cycle for the transpiration rate over 10 min. The transpiration rates were determined by multiplying the flow rate through the cuvette by the difference in humidity between the ingoing and outgoing air.

Sufficient pneumatic pressure (the 'balancing pressure' $P$) was applied in the root chamber to bring the exposed xylem in a trimmed leaf to the point of bleeding (Fig. S1d). Nulsen *et al.* (1977) have shown that this pressure is numerically equal to the suction that would have existed in the xylem had the roots not been pressurized. Plants were kept at balancing pressure as the soil dried by an automatic electronic controller. A sensor attached to the trimmed leaf transmitted a signal to the controller which regulated the chamber pressure to maintain the xylem sap at the point of bleeding, with a precision of *c.* 5 kPa and a range from 0 to 2400 kPa.

A typical experiment consisted in the application of a cycle of five stages of increasing evaporative demand (Table 1), followed by four stages of decreasing demand. The initial conditions were a vapor pressure deficit (VPD) of 0.3 kPa (giving a relative humidity (RH) of *c.* 90%) and a light intensity of 50 μmol $m^{-2}$ $s^{-1}$ of photosynthetically active radiation (PAR). The largest evaporative demand had a VPD of 1.3 kPa (with RH of *c.* 50%) and a PAR of 600 μmol $m^{-2}$ $s^{-1}$. The intermediate stages were established by changing either or both of the humidity in the chamber and the light intensity. Each cycle lasted *c.* 6 h. The cycle was shortened in dry soils when the balancing pressure $P$ reached 2400 kPa before stage 5. During this time, the

**Table 1** Environmental conditions in the cuvette at the five stages of increasing evaporative demand

| Stage | PAR (μmol $m^{-2}$ $s^{-1}$) | Humidity (g $m^{-3}$) | Relative humidity (%) |
|---|---|---|---|
| 1 | 50 | 19 | 90 |
| 2 | 100 | 15 | 70 |
| 3 | 100 | 13 | 60 |
| 4 | 250 | 11 | 50 |
| 5 | 600 | 11 | 50 |

The stages for decreasing evaporative demand were in reverse (that is: ordered as 4, 3, 2 and 1) to yield nine stages in total for a single full cycle. PAR, photosynthetically active radiation.

© 2017 The Authors
*New Phytologist* © 2017 New Phytologist Trust

electronic pressure controller maintained the system automatically at balancing pressure, and the pot was maintained at a constant temperature to ensure that the viscosity of the flowing water remained constant. We chose a temperature of 13°C which is similar to that experienced by young barley plants in the field. A complete set of measurements involved measuring the relationship between the balancing pressure $P$ and the transpiration rate $E$ for cycles of increasing and decreasing transpiration rate and for decreasing water contents over several days as the soil dried. A full set of measurements lasted *c.* 10 d during which wild-type and *brb* mutant plants were alternated in the chamber.

The average soil water content in each pot was measured gravimetrically at the beginning and end of its time in the pressure chamber, and the loss in water agreed well with the integration of the transpiration rate during that time.

At the end of each set of measurements, the soil in the pot was gently washed out, roots were stored in ethanol : water (50 : 50 v/v) and gross root morphologies were analyzed. Stored roots were floated in a plastic tray and scanned using a flatbed scanner (Epson Expression 800; Epson Australia, Sydney, NSW, Australia) at a resolution of 400 dpi. Total root lengths, average root diameters and surface areas (excluding root hairs) were measured with WinRhizo Pro v.2002 (Regent Instruments Inc., Quebec, QC, Canada). Root hair length was measured according to Delhaize *et al.* (2012). Specific root length (root length per root fresh weight) was calculated using the average root radius and the total root length to calculate the root volume, and by assuming that the fresh root density was 1 g $cm^{-3}$.

### Replication

The experiments were replicated three times per genotype in the sandy loam potting mix and twice per genotype in the Red Chromosol. Overall, we measured five wild-type plants and five mutants. Each individual was measured at a minimum of two different water contents. For the statistical analysis of the $P(E)$ curves (Table 1), we used data only from pairs of genotypes at the same soil water content, with comparisons not confounded by differing soil water contents, so that each individual plant was counted only once ($n = 5$) for the calculations.

Root morphology (total length and diameter) was measured only for the plants grown in the sandy loam potting mix ($n = 3$), as the pots of the Red Chromosol were reused for other experiments.

### Numerical simulation

To explore the hypothesis that root hairs facilitate water uptake, we used a numerical model to simulate the radial flow of soil water. The aim of the simulation was not to describe in detail the uptake of water by root hairs, which would require a more sophisticated model, such as that used for phosphate uptake by Keyes *et al.* (2013), but to test whether the observed dynamics of $P(E)$ could, to a first approximation, be explained by the principles of the radial flow of water towards the root surface, along the lines of Gardner's (1960) model.

Water flow in soil was simulated by solving the Richards' equation in radial coordinates:

$$\frac{\partial \theta}{\partial t} = \frac{1}{r}\frac{\partial}{\partial r}\left[rk(h)\frac{dh}{dr}\right] \quad \text{Eqn 1}$$

where $\theta$ is the volumetric water content ($m^3\ m^{-3}$), $h$ is the soil matric potential (Pa), $k$ is the soil hydraulic conductivity ($m^2\ s^{-1}\ Pa^{-1}$), $r$ is the radial coordinate (m) and $t$ is time (s). When the soil matric potential is expressed as matric head $h/\rho g$ (m) (where $\rho$ is the water density and $g$ is gravity), the soil hydraulic conductivity $k$ has the units of ($m\ s^{-1}$).

It is assumed that each root of radius $a$ has sole access to a cylinder of outer radius $b = 1/\sqrt{\pi L}$, where $L$ is the root length density ($m\ m^{-3}$). It is further assumed that $L$ is uniform throughout the soil columns and that water uptake is uniform along the root system. The boundary conditions are zero flow at the outer radius $b$, whereas the rate of uptake per unit length ($m^3\ m^{-1}\ s^{-1}$) is calculated by dividing the measured transpiration rate by the active fraction of the root length. The parameter to be fitted for the hairless mutant was the active fraction of the total root length (from which we derived the active length $L$). For the wild-type, we kept $L$ constant, and the only parameter that was varied was the 'effective' root radius $a$, which is the effective radius of the root epidermis plus the length of the root hairs.

The soil parameters and a more detailed description of the model are given in Methods S1.

## Results and Discussion

The hydraulic properties of the two soils are plotted in Fig. 2. The potting mix had a higher gravimetric water content than the Red Chromosol at any given matric potential. The potting mix showed a large decrease in water content between −2 and −10 kPa, which corresponds to the drainage of relatively large pores with diameters of *c.* 30–150 μm. The unsaturated hydraulic conductivity of the potting mix was less than that of the Red Chromosol. Qualitative visual inspection of the potting mix revealed that it was largely made up of micro-aggregates (i.e. porous grains), which explains the high water retention, as well as the large drop in water content between −2 and −10 kPa. The poor hydraulic contact between the micro-aggregates explains the low hydraulic conductivity of this soil at low matric potentials.

Figure 3 shows a representative experiment in which a *brb* mutant was directly compared with a wild-type plant (cv Pallas) growing in the sandy loam potting mix at a gravimetric water content of $\theta_g = 0.17$ and matric potential of $h = -50$ kPa. The pots were placed in the root pressure chamber in the morning with low evaporative demand. During the day, the transpiration rate was increased in five steps and then decreased stepwise over 5–6 h (Fig. 3a). At low $E$, the *brb* mutant and wild-type plants had similar balancing pressures that showed a linear relationship for $P(E)$ (stages 1–4). When $E$ was increased to *c.* 450 μg $s^{-1}$ (stage 5), $P$ for the *brb* mutant started to increase rapidly despite $E$ remaining essentially constant (indicated by an arrow in Fig. 3b). By contrast, $P$ increased much more slowly for the



© 2017 The Authors
*New Phytologist* © 2017 New Phytologist Trust

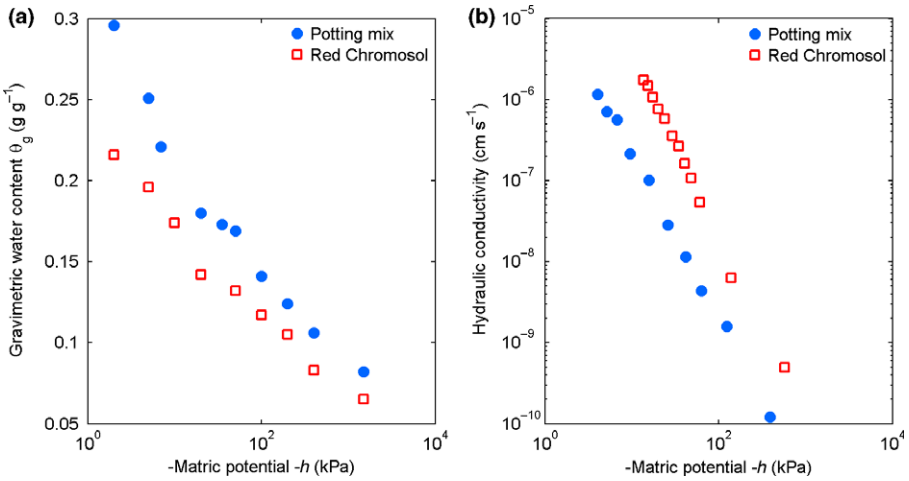


**Fig. 2** Soil hydraulic properties. (a) Water retention curve of the potting mix and the Red Chromosol as measured with the pressure plate apparatus. (b) Unsaturated hydraulic conductivity of the potting mix and the Red Chromosol measured using the evaporation method (Peters & Durner, 2008). The points shown here were obtained by interpolation. For the simulations shown in Fig. 6, the water loss and matric potentials during evaporation were fitted using the Richards equation (Eqn 1) to inversely estimate the unsaturated hydraulic conductivity.

wild-type plant at the same $E$. When the transpiration was reduced, the $P(E)$ curves were parallel to the initial curves generated by increasing $E$. $P$ then slowly decreased to approach the initial curve at the lowest transpiration rate.

Figure 3(c) shows that $P(E)$ was predominantly linear at low transpiration rates during the phase of increase and can be described as:

$$P = R \cdot E + P_0 \qquad \text{Eqn 2}$$

where $P_0$ is the intercept on the $P$ axis and $R$ is the slope of the curve, which has been interpreted as the hydraulic resistance of the plant (Passioura, 1980). We later refer to the deviation of $P$ from the extrapolated linear relationship as $\Delta P$ (Fig. 3c).

Whereas Fig. 3 illustrates a large difference in the behavior of the genotypes at a given transpiration rate, Fig. 4 illustrates that the wild-type can maintain a substantially higher transpiration rate than the mutant at a given moderately low soil water potential. The plants used to generate Fig. 3 were measured again 2 d later when $\theta_g = 0.15$ (Fig. 4a). $P_0$ at the start of the experiment was *c.* 1000 kPa, which is *c.* 400–500 kPa higher than that at $\theta_g = 0.17$. When $E$ was increased to *c.* 250 μg $s^{-1}$ (from stage 2 to 3), the $P(E)$ curves for both genotypes were parallel to the curves measured at $\theta_g = 0.17$. At stage 3, $P$ remained relatively constant

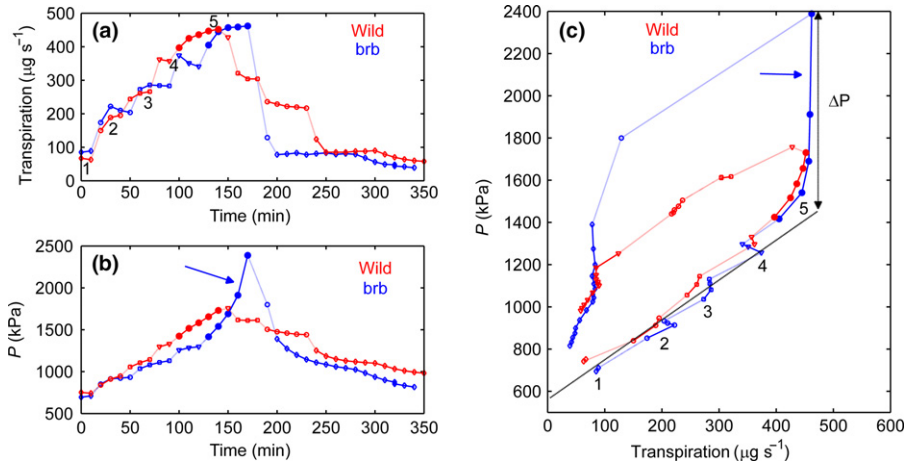


**Fig. 3** Comparison of a root-hairless barley *brb* (*Hordeum vulgare*) mutant and its wild-type plant during one experimental cycle in the sandy loam potting mix. The data shown were collected from a *brb* and a wild-type plant grown in the sandy loam potting mix at an initial gravimetric water content of $\theta_g = 0.17$. (a) One cycle of increasing and decreasing transpiration when the plants were placed in the root pressure chamber. Transpiration was modified by varying the humidity and light intensity. The numbers below the plots indicate the staged increases (Table 1) in transpiration rate. The measurements were logged at 10-min intervals (although the two points that follow a large change in humidity are not shown because the change in the humidity of the ingoing air takes *c.* 20 min to settle). Points with the same symbol connected by solid lines refer to the same stage. Points connected by the light, dotted line refer to the transition between the stages. (b) Balancing pressure $P$ needed to maintain the leaf xylem at atmospheric pressure. The balancing pressure is numerically equal to the suction that the xylem would have had if the plant had not been pressurized. The time is identical to that in plot (a). The blue arrow indicates the large increase in $P$ in *brb* under high transpiration demand. (c) Relationship between $P$ and $E$. At low transpiration stages (1–4), the $P(E)$ curves for the two genotypes were similar and linear. At stage 5, there was a rapid increase in $P$ in *brb* (blue arrow), compared with the moderate increase in the wild-type. The deviation of $P$ from the linear relationship is referred to as $\Delta P$.

© 2017 The Authors
*New Phytologist* © 2017 New Phytologist Trust

New Phytologist

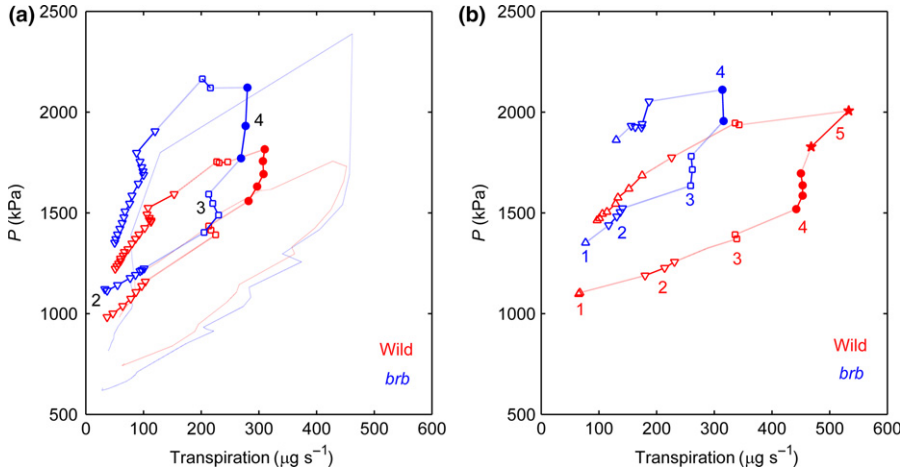


**Fig. 4** Comparison of a root-hairless barley *brb* (*Hordeum vulgare*) mutant and its wild-type plant in the sandy loam potting mix. (a) Relationship between balancing pressure (*P*) and transpiration rate (*E*) for the same plants as shown in Fig. 3, measured 2 d later when the gravimetric water content had fallen to $\theta_g = 0.15$. The thin lines without symbols refer to the *P*(*E*) curves measured at $\theta_g = 0.17$ (Fig. 2c). The numbers refer to increasing transpiration stages (in these measurements, we started at stage 2). Compared with the wetter samples, the deviation of *P* from the straight line occurred at lower *E*. As in Fig. 3, *P* increased more rapidly in the *brb* mutant. (b) Comparison of a *brb* mutant with a wild-type plant grown in the potting mix at $\theta_g = 0.14$ (different plants from Fig. 4a). For the *brb* hairless mutant, the balancing pressure *P* started to increase more rapidly at intermediate transpiration conditions (stage 3), whereas higher transpiration rates could be sustained by the wild-type before *P* increased (stage 5). Stage 4 was selected for both pairs of samples to calculate $\Delta P$ for Fig. 6.

for the wild-type, whereas it started to increase in the mutant. When *E* was further increased to *c.* 300 μg $s^{-1}$ (stage 4), *P* started to increase rapidly for the mutant. The increase was so rapid that the transpiration had to be reduced after 30 min to avoid exceeding the range of the pressure controller. Even when the transpiration was decreased to *c.* 200 μg $s^{-1}$, *P* continued to increase. *P* started to decrease only when *E* was further decreased to the initial values (stages 1–2). By contrast, the wild-type showed an almost linear *P*(*E*) relationship as transpiration was decreased after the *P* maximum had been reached. In addition, it showed a more moderate deviation ($\Delta P$) from a projection of the linear line over the same time of 20 min, despite being exposed to a larger maximum transpiration rate ($E > 300$ μg $s^{-1}$) than the mutant.

Similarly, Fig. 4(b) shows the *P*(*E*) relationship for two other plants grown in the sandy loam potting mix at $\theta_g = 0.14$ ($h = -100$ kPa). When the transpiration rate was increased to *c.* 260 μg $s^{-1}$ (stage 3), the balancing pressure *P* for the mutant started to increase rapidly. By stage 4, *P* continued to increase (*c.* 150 kPa in 10 min). By contrast, for the wild-type plant, *P* was constant at stage 3 and started to increase only at stage 4 ($E \approx 450$ μg $s^{-1}$) and more slowly than did the mutant. As *P* for the wild-type plant was still < 2.4 MPa after stage 4, the transpiration rate could be increased further. By stage 5, *P* for the wild-type increased rapidly; however, at this stage, the transpiration rate was 70% higher than that at stage 3, where *brb* showed a similar rapid rise in *P*.

Figure 5 shows a representative set of experiments made with the two genotypes growing in the Red Chromosol soil as it dried over several days. When the soil was wet ($\theta_g = 0.15$), *P*(*E*) was linear. In drier soils, *P*(*E*) remained linear for low *E*, but, when *E* was large, *P* deviated upwards from the projected line. This deviation $\Delta P$ was substantially greater in the hairless mutant than in the wild-type. The measurements with the Red Chromosol confirmed in qualitative terms the experiments in the sandy loam potting mix. Additional measurements are shown in Figs S2–S5.

Notably, in the Red Chromosol, *P* started to deviate from the linear relationship at lower water contents compared with the experiments in the sandy loam potting mix. At $\theta_g = 0.11$ (corresponding to a matric potential $h \approx -200$ kPa), both the wild-type and the hairless mutant reached the transpiration rate of

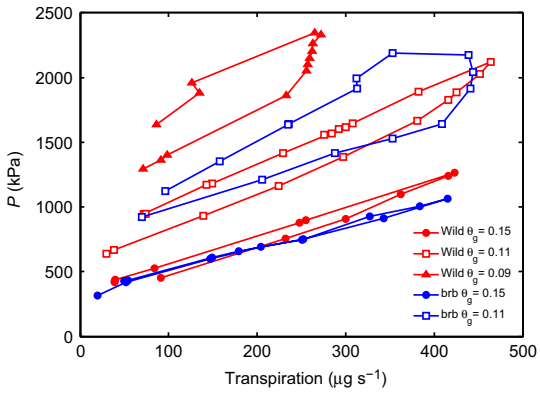


**Fig. 5** Comparison of a root-hairless barley *brb* (*Hordeum vulgare*) mutant and its wild-type plant in the Red Chromosol. Relationship between balancing pressure (*P*) and transpiration rate (*E*) for two genotypes at varying soil water contents. In wet soil ($\theta_g = 0.15$), *P*(*E*) was linear and similar in both genotypes. In drier soils, *P*(*E*) was linear for low *E*, but, when *E* was large, *P* deviated upwards from the projected line. This deviation $\Delta P$ was substantially greater in the hairless mutant than in the wild-type. For the wild-type at $\theta_g = 0.09$, the *P*(*E*) relationship was linear and approximately parallel to the curves in wet soil until a transpiration rate of *c.* 200 μg $s^{-1}$ was attained. At higher transpiration rates, *P* started to deviate from the linear relationship.



© 2017 The Authors
*New Phytologist* © 2017 New Phytologist Trust

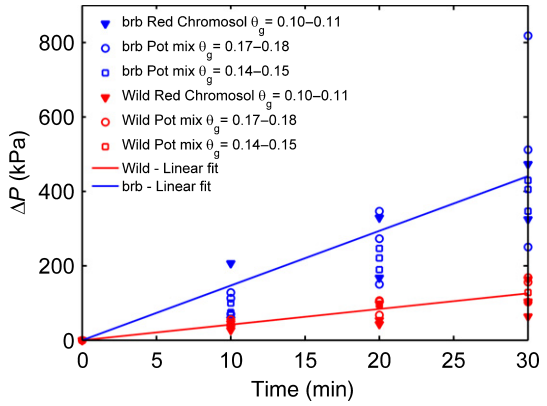


**Fig. 6** Difference between the balancing pressure (*P*) required at high transpiration rates and the linear phase of the *P*(*E*) relationship, $P = R{\cdot}E + P_0$. $\Delta P$ was estimated in samples for which a direct comparison between barley (*Hordeum vulgare* brb mutant and wild-type) genotypes was permissible, that is at the water contents and transpiration stage for which we had three replicates per genotype in the potting mix and two replicates per genotype in the Red Chromosol, and for which the transpiration stage was imposed for at least 20 min. The samples used to calculate $\Delta P$ are shown in Fig. 3 (stage 5), Fig. 4(a,b) (stage 4) and Supporting Information Figs S3–S5 (stages indicated by an arrow). The solid lines are the best linear fits of the two genotypes independent of water content, transpiration rate and soil type.

400–500 $\mu g\ s^{-1}$, although this resulted in a rapid rise in *P* in the hairless mutant (Fig. 5). In the sandy loam potting mix, this transpiration rate could be sustained by both genotypes only at $\theta_g \geq 0.17$ ($h \approx -50$ kPa) (Figs 3, 4a). It should be noted that the sandy loam potting mix at $\theta_g = 0.17$ and the Red Chromosol at $\theta_g = 0.11$ had a similar hydraulic conductivity of $k \approx 5 \times 10^{-9}$ ($cm\ s^{-1}$), which suggests that the deviation of *P* from the linear relationship (Eqn 2) is related to the soil hydraulic conductivity – that is the deviation of *P* occurs when the soil is no longer able to conduct water fast enough to sustain the transpiration demand.

Figure 6 summarizes all data collected for the two soils for which the *brb* mutant could be directly compared with the wild-type based on similar soil water contents and transpiration rates. The figure shows how rapidly *P* deviated from the linear relationship at high transpiration rates. *R* and $P_0$ were estimated by fitting Eqn 2 to the initial part of the measured *P*(*E*) relationship. $\Delta P$ was calculated as the difference between the measured *P*(*E*) and the extrapolated linear fit (Fig. 3c). $\Delta P$ increased approximately linearly over time. The average slope of $\Delta P$ over time ($\Delta P/\Delta t$) was 2.75-fold greater in the *brb* mutant than in the wild-type (Table 2). The figure illustrates that, at transpiration rates at which *P* started to rapidly deviate from the initial linear phase of the curve, this occurred faster for *brb* mutants than for the wild-type plants over all the experiments (Table 2; $P = 0.002$, $n = 5$).

The root hair lengths were 0.64 and 0.83 mm for thin and coarse roots in the wild-type, whereas the root hair length was null in the *brb* mutant (Table 2). The measured root hair lengths fitted well with the values reported in the literature. Root hairs of wild-type Pallas were found to have an average length of 1 mm (Haling *et al.*, 2010) when grown in a ferrosol. In different studies, Brown *et al.* (2012) found that the barley cultivar Optic had

**Table 2** Root properties and associated *P* values of two genotypes of barley (*Hordeum vulgare*), the root-hairless *brb* mutant and its wild-type (data show means ± SD)

| | Root diameter (mm) ($n = 3$) | Total length coarse roots (m) ($n = 3$)[a] | Total length fine roots (m) ($n = 3$)[b] | Root hair length coarse roots (mm) ($n = 3$) | Root hair length fine roots (mm) ($n = 3$) | Specific root length ($m\ g^{-1}$) ($n = 3$)[d] | Plant hydraulic resistance *R* ($kPa\ \mu g^{-1}\ s$) ($n = 5$)[e] | $\Delta P/dt$ ($kPa\ min^{-1}$) ($n = 5$)[f] |
|---|---|---|---|---|---|---|---|---|
| *brb* mutant | 0.26 ± 0.02 | 4.2 ± 0.3 | 32.4 ± 9.9 | 0 ± 0 | 0 ± 0 | 19.3 ± 2.4 | 1.8 ± 0.6 | 13.2 ± 1.8 |
| Wild-type | 0.31 ± 0.03 | 5.5 ± 1.2 | 27.6 ± 11.7 | 0.83 ± 0.06 | 0.64 ± 0.18 | 13.6 ± 2.5 | 2.3 ± 0.5 | 4.8 ± 1 |
| *P* value, two-tailed *t*-test | 0.09 | 0.15 | 0.62 | < 0.01 | < 0.05 | 0.047 | 0.2 | 0.002 |

[a]Coarse roots are defined as having diameters of > 0.36 mm.
[b]Fine roots are defined as having diameters of < 0.36 mm.
[c]Root hair length was measured according to Delhaize *et al.* (2012).
[d]Specific root length was calculated using the average root radius and the total root length to calculate the root volume assuming that root density was 1 $g\ cm^{-3}$.
[e]The plant hydraulic resistance (*R*) was calculated by fitting the linear part of the *P*(*E*) curves and included data for plants grown in both soils.
[f]$\Delta P/dt$ is the deviation of *P* from the linear *P*(*E*) relationship over time. It was calculated for both soils: the sandy loam potting mix at $\theta_g = 0.14$–0.15 and the Red Chromosol at $\theta_g = 0.10$–0.11 (each individual plant was counted only once for each soil, $n = 5$ in total for both soils). $\Delta P/dt$ was calculated from Fig. 6.

© 2017 The Authors
*New Phytologist* © 2017 New Phytologist Trust

root hairs *c.* 0.8 mm long, and Gahoonia *et al.* (1999) showed that barley cultivars grown under a variety of conditions, including 25 d in the field, had root hairs ranging from 0.5 to 1.0 mm.

Total root lengths, average root diameters, surface areas (excluding root hairs) and plant hydraulic resistances were not significantly different between the wild-type and the hairless mutant (Table 2). However, calculated specific root lengths differed significantly ($P < 0.05$, Table 2), with the *brb* mutant having a larger specific root length when the genotypes grown on the sandy loam potting mix were compared. This difference in specific root length can be attributed to the *brb* mutant having thinner roots than the wild-type (Table 2; although $P > 0.05$), as reported by Genc *et al.* (2007). A greater specific length might be a compensatory response of the mutant to not having hairs, as proposed by Dodd & Diatloff (2016), but clearly this was not sufficient to sustain the high transpiration rates in drying soils. Furthermore, Genc *et al.* (2007) argued that the root hairs can make the roots appear thicker when scans are analyzed by software, such as WhinRhizo, as it does not take root hairs into account. Root hairs can clump and adhere to the root, thus increasing the apparent root diameter, and the smaller diameter of the *brb* mutant could be an artifact of the analytical method. In any case, even if the roots of *brb* are thinner by *c.* 0.05 mm, as found here, this will have a relatively small effect on the total root diameter and water uptake, considering that the diameter of the root hairs and root is *c.* 1.7 mm for the wild-type (assuming a root hair length of 0.7 mm) and only *c.* 0.3 mm for the *brb* mutant.

The deviation of the balancing pressure $P$ from the linear relationship between $P$ and $E$ expressed by Eqn 2, $\Delta P$, has been interpreted as a drop in matric potential between the bulk soil and the surface of a root (Passioura, 1980). Small upward deviations could arise from the soil drying during the experiment, thus leading to a fall in the matric potential of the bulk soil. However, at the end of each cycle of increasing and decreasing transpiration rate, $P$ decreased and approached the value at the beginning of the cycle. More likely, the vertical trajectories of $P(E)$ for the root-hairless mutant can be interpreted as the decrease in matric potential at the root–soil interface when the limiting uptake rate is reached. Alternatively, or additionally, the rapid rise in $P$ might be caused by the accumulation of solutes at the root–soil interface when the convective fluxes are much larger than the back diffusion of the solutes, with a consequent decrease in the osmotic potential at the root–soil interface, as discussed later in the text.

The numerical simulations shown in Fig. 7 support the interpretation that the rapid increase in $P$ at high transpiration rates corresponds to a drop in water potential in the first millimeter around the roots, and that this drop in water potential is attenuated when the root radius is extended to account for water uptake by the root hairs. As a representative fit of the experimental data, we chose one wild-type plant and a *brb* plant in the sandy loam potting mix at $\theta_g = 0.14$ (Fig. 4b). However, when simulating the gradients with $\theta_g = 0.14$, no gradients were generated in soil matric potential and $P(E)$ was linear. A reasonable fit was obtained only when the active root length was reduced to *c.* 40 cm, which is only 1% of the root length and is probably an underestimation of the active root length. Therefore, $\theta_g$ was

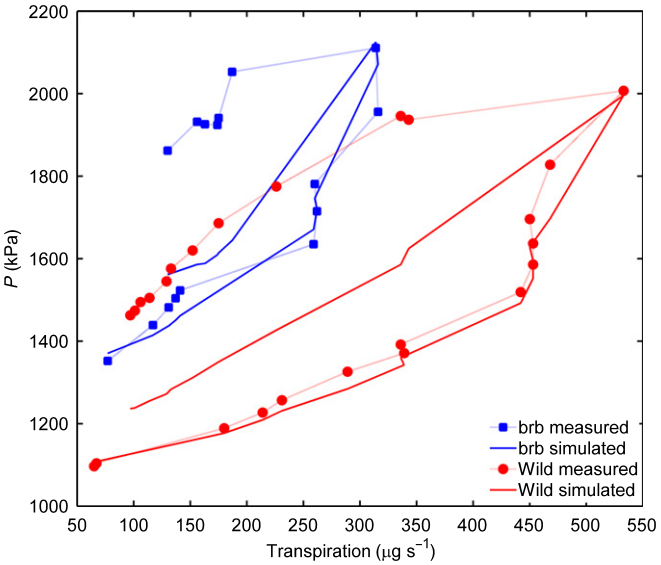


**Fig. 7** Numerical simulations of root water uptake. Simulations of the $P(E)$ curves of the *brb* mutant (*Hordeum vulgare*) and wild-type plant in the potting mix at $\theta_g = 0.14$ (same samples as shown in Fig. 4b). The simulations gave the soil matric potential experienced by the roots added to the linear part of the $P(E)$ curve, $R \cdot E + P_0$ (Eqn 2), which represents the drop in pressure within the plant. The active root length was taken to be 300 cm. The effect of root hairs was simulated by extending the root radius from 0.13 mm (root radius without hairs) to 0.7 mm (root radius plus root hair length). Simulations reproduced the experimental data well during the period in which the transpiration $E$ was increased. However, the simulations predicted a much faster decrease in the balancing pressure $P$ after $E$ was decreased.

decreased from 0.14 to 0.12 for the simulation and the best fit for the *brb* mutant was obtained using an active root length equal to 300 cm, which was *c.* 10% of the total root length. The improvement obtained using the altered $\theta_g$ parameter might be caused by the water not being evenly distributed throughout the soil – although the pots had high roots densities throughout their volume. For the wild-type plants, the best fit was obtained by extending the root radius to 0.7 mm to include root hairs (compared with 0.13 mm of the hairless mutant), whilst keeping the same root length and water content. The extension of the root radius to 0.7 mm fits well with the measured hair length of 0.64–0.83 mm.

Under the assumptions that only 10% of the root length takes up water and that $\theta_g$ could be reduced from 0.14 to 0.12, the simulated gradients in soil matric potentials fit well with the observed $\Delta P$ during the increasing transpiration phase, and extending the root radius reproduced well the differences between the roots with and without hairs. The need to reduce the active root length to 10% and $\theta_g$ from 0.14 to 0.12 shows the difficulties in fitting the $P(E)$ curve using a cylindrical model of water flow to a representative single root (Eqn 1) and assuming that the properties of the soil around the roots are homogeneous. Similar conclusions were reached when simulating other experiments (e.g. Fig. S6). Even more challenging is the fact that the simulations were not able to reproduce the $P(E)$ relationship during the phase of decreasing transpiration rates. The simulations predicted a rapid decrease in $P$ on relaxation of the transpiration rate and



© 2017 The Authors
*New Phytologist* © 2017 New Phytologist Trust

were not able to fit the slow recovery of *P*. Such apparent hysteresis of the *P*(*E*) curves confirms former experiments (Passioura, 1980; Deery *et al.*, 2013), but its explanation remains a puzzle.

## General discussion

Our experiments using the root chamber technique have shown that root hairs can facilitate water uptake by plants experiencing high transpiration rates in drying soils. The balancing pressures *P* at high transpiration rates *E* in moderately dry soil were much greater in the hairless mutants than in the wild-types (Figs 3–5). In wet soil, and at low *E* in moderately dry soil, *P*(*E*) was predominantly linear (Figs 5, S2). Its slope is the hydraulic resistance of the plant (Eqn 2), because gradients in pressure in the soil are small in these circumstances.

The different behaviors shown by the wild-type and hairless mutant in Figs 4 and 5 are supportive evidence of the hypothesis outlined in Fig. 1. This is reinforced by the accuracy of the numerical model for water flow to a root in predicting the major potential at the surface of a hairless root and at the surface of a notional coaxial cylinder enclosing the root hairs of wild-type plants. However, the large hysteresis evident in Figs 3–5 when *E* is being reduced cannot be accounted for by the model. Some process in addition to that described by the simple physical model of radial water transport in soil to a root is likely to be responsible. Furthermore, the intercept on the *y*-axis of the linear part of the *P*(*E*) curves, *P0*, should, in a simple physical model, approximate to the matric potential of the bulk soil, but it does not. How can we explain these two large discrepancies?

**Hysteresis of the *P*(*E*) curves** The hysteresis has been noted previously by Passioura (1980) and Deery *et al.* (2013), although without a convincing explanation. One possibility is that large gradients in osmotic potential develop close to the surface of roots that are taking up water but not solutes. Stirzaker & Passioura (1996) postulated this in trying to explain why the water relations of a barley plant growing in well-fertilized soil changed greatly when the soluble nutrients had been leached out. In the well-fertilized soil, in which the soil solution had a substantial osmotic pressure (perhaps 100 kPa), *P* rose rapidly when *E* was large, but did not do so in the leached soil. McCully (1994, 1995) argued that the uptake of water and nutrients may be spatially separated in roots. If this is the case, a combined model of water and solute flow would be needed to explore the phenomenon. Both the potting mix and the field soil used in our experiments were well fertilized.

Another possible explanation of the hysteresis is that the hydraulic properties of the zone close to the root are not the same as those of the bulk soil and are time-dependent. These hydraulic properties are affected by the presence of mucilage released from roots (Carminati, 2012; Kroener *et al.*, 2014). Mucilage increases the soil water retention, maintaining the rhizosphere wet and possibly conductive as the soil dries (Ahmed *et al.*, 2014). However, mucilage and rhizosphere turn water repellent on drying, temporarily limiting the recovery of the rhizosphere hydraulic conductivity after the soil is rewetted (Zarebanadkouki *et al.*, 2016). At high transpiration rates, water extraction from the mucilage-embedded rhizosphere might exceed water flow from the bulk soil, such that the first millimeters of soil around the roots are rapidly depleted of water. This would result in a rapid decrease in water potential at the root–soil interface which, in our experiments, would appear as a vertical trajectory in the *P*(*E*) curve. When *E* is decreased, the recovery in water content and matric potential at the root–soil interface would lag behind because of the slow rewetting rate of the rhizosphere, resulting in hysteresis in *P*(*E*). Currently, there is still little information on the hydraulic properties of the rhizosphere and this explanation remains speculative. However, it is intriguing that both the rhizosphere water content and the relation between *P*(*E*) show a strong hysteresis.

A third possibility is that the water in the pots was unevenly distributed. Couvreur *et al.* (2012) showed mathematically that the soil water potential experienced by the plant should correspond to the average soil water potential weighted according to the local root water uptake. For example, if the roots in the top third of the pot were dominating the uptake of water, the matric potential in the soil region they occupy might fall rapidly when *E* is large, resulting in a rise in *P*. Subsequent redistribution of water from the bottom two-thirds of the pot to the top third when *E* is reduced could account for the hysteresis, as it happens over a much larger distance than the replenishment of water adjacent to the root surface (about 100-fold; *c.* 100 mm compared with *c.* 1 mm), and thus requires much longer to equilibrate. We have no data on water distribution in the pots, but this explanation seems unlikely because: (1) the roots were fairly evenly distributed in the pots (visual observations); (2) the hysteresis appeared even in relatively wet soils ($\theta_g = 0.18$, corresponding to a soil matric potential of −10 kPa; Fig. S2), when the soil hydraulic conductivity (Fig. 2) was sufficiently high to quickly reduce even large gradients in soil water potentials; (3) simulations of water flow in the soil column, assuming a linear decrease in root water uptake with depth and no root water uptake at the bottom, predict a local decrease in matric potential at the top of the soil during the transpiration cycle, but this decrease is much smaller than the measured rise in *P* (Notes S1, Figs S7, S8).

A fourth possible explanation for the hysteresis is that the roots might have shrunk, thereby causing loss of contact between soil and roots and the formation of air-filled gaps at the root–soil interface (Huck *et al.*, 1970; Carminati *et al.*, 2013). Hysteresis may have been associated with the rehydration of shrunken roots.

**Why does the balancing pressure not relax further during the night so that $P_0$ remains very high?** A final puzzle concerns the large values of *P* at the start of each experiment. After a night of little transpiration in a soil at a matric potential of −50 kPa (nominal average for the plant discussed in Fig. 3), it was surprising to find that $P_0$ was *c.* 500 kPa. Similarly surprising was that $P_0$ was *c.* 1000 kPa when the soil matric potential was *c.* −100 kPa (Fig. 4). The simple expectation is that $P_0$ would approximate the water potential in the bulk soil, including its matric and osmotic components. This was so in the experiments of Passioura (1980) and in similar experiments with barley in

© 2017 The Authors
*New Phytologist* © 2017 New Phytologist Trust

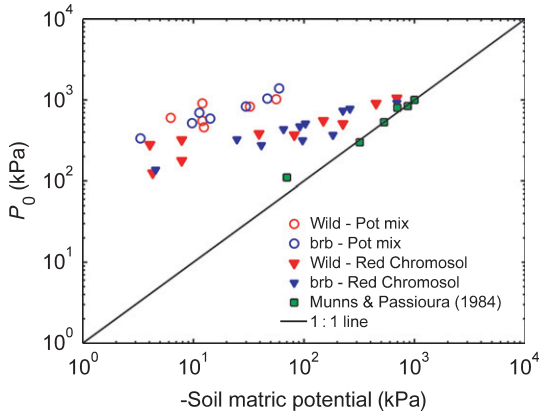


**Fig. 8** Intercept of the *P*(*E*) curve ($P_0$) vs the soil matric potential at the beginning of each measurement for root-hairless barley *brb* (*Hordeum vulgare*) mutant and its wild-type. $P_0$ was mostly greater than the expected soil suction, especially in wet soils. The difference is reduced in dry soils. For comparison, we also added $P_0$ and the varied osmotic potential of the soil solution of an experiment by Munns & Passioura (1984) using sand culture.

sand culture in which the NaCl concentration was varied to give a range of osmotic pressures in the nutrient solution from 70 to 1000 kPa (Munns & Passioura, 1984). In Fig. 8 the relationship between *P0* and the soil matric potential is plotted for all the experiments. For comparison we also included *P0* and the osmotic potential of the soil solution of the experiment of Munns & Passioura (1984). In our experiments, there was a large variation between $P_0$ and the soil matric potential. The difference in wet soil ($h > -10$ kPa) can be interpreted as the osmotic pressure of the soil solution, which is likely to be in the range of 100–150 kPa in a fertile soil. Thus, the differences that were much larger than this presumably imply that the roots were experiencing a large additional osmotic pressure at their surface or possibly within the apoplast of the cortex (Stirzaker & Passioura, 1996).

In conclusion, our results show that wild-type barley is substantially more effective than the *brb* mutant at taking up water from moderately dry soil, thereby supporting the view that root hairs play an important role in the uptake of water from a drying soil. In addition, the results strongly reinforce earlier observations that: (1) there is a marked hysteresis in balancing pressure (the suction in the xylem) when the transpiration rate is rising compared with when it is falling; and (2) that this hysteresis remains after a night of very low transpiration rate, possibly because of a residual buildup of osmotic pressure at the surface of the roots. These conundrums remain a major challenge to our understanding.

## Acknowledgements

The McMaster fellowship (CSIRO) is acknowledged for funding the research stay of A.C. at CSIRO, Canberra, Australia.

## Author contributions

E.D., J.B.P., M.W. and A.C. designed the study; A.C. and J.B.P. performed the experiments; M.Z. and A.C. made the numerical simulations; A.C. analyzed the data; J.B.P., A.C., M.Z. and M.A.A. measured the soil properties; A.C., J.B.P., E.D., P.R.R. and M.W. wrote the text; all authors read and commented on the text.

## References

**Ahmed MA, Kroener E, Holz M, Zarebanadkouki M, Carminati A. 2014.** Mucilage exudation facilitates root water uptake in dry soils. *Functional Plant Biology* **41**: 1129–1137.

**Bates TR, Lynch JP. 2001.** Root hairs confer a competitive advantage under low phosphorus availability. *Plant and Soil* **236**: 243–250.

**Bristow CE, Campbell GS, Wullstein LH, Neilson R. 1985.** Water uptake and storage by rhizosheaths of *Oryzopsis hymenoides*: a numerical simulation. *Physiologia Plantarum* **65**: 228–232.

**Brown LK, George TS, Thompson JA, Wright G, Lyon J, Dupuy L, Hubbard SF, White PJ. 2012.** What are the implications of variation in root hair length on tolerance to phosphorus deficiency in combination with water stress in barley (*Hordeum vulgare*)? *Annals of Botany* **110**: 319–328.

**Cailloux M. 1972.** Metabolism and the absorption of water by root hairs. *Canadian Journal of Botany* **50**: 557–573.

**Carminati A. 2012.** A model of root water uptake coupled with rhizosphere dynamics. *Vadose Zone Journal* **11**. doi: 10.2136/vzj2011.0106

**Carminati A, Vetterlein D, Koebernick N, Blaser S, Weller U, Vogel H-J. 2013.** Do roots mind the gap? *Plant and Soil* **367**: 651–661.

**Couvreur V, Vanderborght J, Javaux M. 2012.** A simple three-dimensional macroscopic root water uptake model based on the hydraulic architecture approach. *Hydrology and Earth System Sciences* **16**: 2957–2971.

**Deery DM, Passioura JB, Condon JR, Katupitiya A. 2013.** Uptake of water from a Kandosol subsoil. II. Control of water uptake by roots. *Plant and Soil* **368**: 649–667.

**Delhaize E, James RA, Ryan PR. 2012.** Aluminium tolerance of root hairs underlies genotypic differences in rhizosheath size of wheat (*Triticum aestivum*) grown on acid soil. *New Phytologist* **195**: 609–619.

**Dittmer HJ. 1949.** Root hair variations in plant species. *American Journal of Botany* **36**: 152–155.

**Dodd IC, Diatloff E. 2016.** Enhanced root growth of the *brb* (bald root barley) mutant in drying soil allows similar shoot physiological responses to soil water deficit as wild-type plants. *Functional Plant Biology* **43**: 199–206.

**Faiz SMA, Weatherley PE. 1982.** Root contraction in transpiring plants. *New Phytologist* **92**: 333–343.

**Gahoonia TS, Nielsen NE. 2003.** Phosphorus (P) uptake and growth of a root hairless barley mutant (*bald root barley, brb*) and wild type in low- and high-P soils. *Plant, Cell & Environment* **26**: 1759–1766.

**Gahoonia TS, Nielsen NE, Joshi PA, Jahoor A. 2001.** A root hairless barley mutant for elucidating genetics of root hairs and phosphorus uptake. *Plant and Soil* **235**: 211–219.

**Gahoonia TS, Nielsen NE, Lyshede OB. 1999.** Phosphorus (P) acquisition of cereal cultivars in the field at three levels of P fertilization. *Plant and Soil* **211**: 269–281.

**Gardner WR. 1960.** Dynamic aspects of water availability to plants. *Soil Science* **89**: 63–73.

**Genc Y, Huang CY, Langridge P. 2007.** A study of the role of root morphological traits in growth of barley in zinc-deficient soil. *Journal of Experimental Botany* **58**: 2775–2784.

**van Genuchten MT. 1980.** A closed-form equation for predicting the hydraulic conductivity of unsaturated soils. *Soil Science Society of America Journal* **44**: 892–898.

**Haling RE, Brown LK, Bengough AG, Young IM, Hallett PD, White PJ, George TS. 2013.** Root hairs improve root penetration, root–soil contact, and phosphorus acquisition in soils of different strength. *Journal of Experimental Botany* **64**: 3711–3721.

**Haling RE, Simpson RJ, Delhaize E, Hocking PJ, Richardson AE. 2010.** Effect of lime on root growth, morphology and the rhizosheath of cereal seedlings growing in an acid soil. *Plant and Soil* **327**: 199–212.

**Herkelrath WN, Miller EE, Gardner WR. 1977.** Water uptake by plants: II. The root contact model. *Soil Science Society of America Journal* **41**: 1039–1043.



© 2017 The Authors
*New Phytologist* © 2017 New Phytologist Trust

**Huck MG, Klepper B, Taylor HM. 1970.** Diurnal variations in root diameter. *Plant Physiology* **45**: 529.

**Keyes SD, Daly KR, Gostling NJ, Jones DL, Talboys P, Pinzer BR, Boardman R, Sinclair I, Marchant A, Roose T. 2013.** High resolution synchrotron imaging of wheat root hairs growing in soil and image based modelling of phosphate uptake. *New Phytologist* **198**: 1023–1029.

**Kroener E, Zarebanadkouki M, Kaestner A, Carminati A. 2014.** Nonequilibrium water dynamics in the rhizosphere: how mucilage affects water flow in soils. *Water Resources Research* **50**: 6479–6495.

**Lang ARG, Gardner WR. 1970.** Limitation to water flux from soils to plants. *Agronomy Journal* **62**: 693–695.

**Marzec M, Melzer M, Szarejko I. 2015.** Root hair development in the grasses: what we already know and what we still need to know. *Plant Physiology* **168**: 407–414.

**McCully M. 1994.** Accumulation of high levels of potassium in the developing xylem elements in roots of soybean and some other dicotyledons. *Protoplasma* **183**: 116–125.

**McCully M. 1995.** How do real roots work – some new views of root structure. *Plant Physiology* **109**: 1–6.

**Munns R, Passioura JB. 1984.** Hydraulic resistance of plants. III. Effects of NaCl in barley and lupin. *Functional Plant Biology* **11**: 351–359.

**Nulsen RA, Thurtell GW, Stevenson KR. 1977.** Response of leaf water potential to pressure changes at root surface of corn plants. *Agronomy Journal* **69**: 951–954.

**Passioura JB. 1980.** The transport of water from soil to shoot in wheat seedlings. *Journal of Experimental Botany* **31**: 333–345.

**Passioura JB. 2006.** The perils of pot experiments. *Functional Plant Biology.* **33**: 1075–1079.

**Passioura JB. 2010.** Plant–water relations. In: *Encyclopedia of life sciences.* Chichester, UK: John Wiley & Sons. [WWW document] URL http://www.els.net/ doi: 10.1002/9780470015902.a0001288.pub2.

**Peters A, Durner W. 2008.** Simplified evaporation method for determining soil hydraulic properties. *Journal of Hydrology* **356**: 147–162.

**Peterson RL, Farquhar ML. 1996.** Root hairs: specialized tubular cells extending root surfaces. *Botanical Review* **62**: 1–40.

**Segal E, Kushnir T, Mualem Y, Shani U. 2008.** Water uptake and hydraulics of the root hair rhizosphere. *Vadose Zone Journal* **7**: 1027.

**Stirzaker RJ, Passioura JB. 1996.** The water relations of the root–soil interface. *Plant, Cell & Environment* **19**: 201–208.

**Suzuki N, Taketa S, Ichii M. 2003.** Morphological and physiological characteristics of a root-hairless mutant in rice (*Oryza sativa* L.). *Plant and Soil* **255**: 9–17.

**Tanaka N, Kato M, Tomioka R, Kurata R, Fukao Y, Aoyama T, Maeshima M. 2014.** Characteristics of a root hair-less line of *Arabidopsis thaliana* under physiological stresses. *Journal of Experimental Botany* **65**: 1497–1512.

**White RG, Kirkegaard JA. 2010.** The distribution and abundance of wheat roots in a dense, structured subsoil – implications for water uptake. *Plant, Cell & Environment* **33**: 133–148.

**Zarebanadkouki M, Ahmed MA, Carminati A. 2016.** Hydraulic conductivity of the root–soil interface of lupin in sandy soil after drying and rewetting. *Plant and Soil* **398**: 267–280.

## Supporting Information

Additional Supporting Information may be found online in the Supporting Information tab for this article:

**Fig. S1** Experimental materials.

**Fig. S2** Relationship between balancing pressure ($P$) and transpiration ($E$) during a drying cycle of a root-hairless barley *brb* (*Hordeum vulgare* L.) mutant grown in the sandy loam potting mix.

**Fig. S3** Relationship between balancing pressure ($P$) and transpiration ($E$) at varying water contents of a root-hairless barley *brb* (*Hordeum vulgare* L.) mutant and its wild-type plant grown in the sandy loam potting mix.

**Fig. S4** Relationship between balancing pressure ($P$) and transpiration ($E$) of a root-hairless barley *brb* (*Hordeum vulgare* L.) mutant and its wild-type plant in the Red Chromosol soil during one cycle of increasing and decreasing transpiration at a gravimetric water content $\theta_g = 0.11$.

**Fig. S5** Relationship between balancing pressure ($P$) and transpiration ($E$) of two additional samples in the Red Chromosol at a gravimetric water content $\theta_g = 0.10$.

**Fig. S6** Simulations of the $P(E)$ curves of a root-hairless barley *brb* (*Hordeum vulgare* L.) mutant and its wild-type plant in the potting mix at $\theta_g = 0.17$ (same samples shown in Fig. 3).

**Fig. S7** Simulations with Hydrus-1D. Imposed transpiration rates.

**Fig. S8** Simulations with Hydrus-1D. Profiles of water content and soil matric potential assuming null root length density and no water uptake at the bottom of the sample.

**Methods S1** Extended description of the numerical simulation.

**Notes S1** Macroscopic simulation of root water uptake and soil redistribution.

Please note: Wiley Blackwell are not responsible for the content or functionality of any Supporting Information supplied by the authors. Any queries (other than missing material) should be directed to the *New Phytologist* Central Office.

© 2017 The Authors
*New Phytologist* © 2017 New Phytologist Trust